*Journal of* ELECTRICAL ENGINEERING, VOL 61. NO 7/s, 2010, 54-57

# MEASUREMENT OF THE TIME-DEPENDENCE OF THE COMPLEX MAGNETIC PERMEABILITY OF SOFT-FERRITES

**Paul Fulmek* — Hannes Wegleiter** — Peter Haumer* — Bernhard Schweighofer****

Ferrimagnetic devices in electrical engineering are usually described by a single complex figure of permeability, which allows deducing simple, but very practical expressions for the inductance in AC considerations. This effective permeability value, however, is dependent on the amplitude of the AC excitation, on the DC magnetic state of the material, and on temperature. Furthermore, it changes considerably with time after the excitation has been applied (magnetic viscosity, magnetic after-effect). In principle, standard measurement systems (impedance/material/network-analyser, LCR-meter) operate under steady-state conditions, after certain settling times have passed. In this paper we describe our measurement system, which is able to characterise the settling process itself, as well. The achieved effective time resolution for the measured impedance values is in the range of 50 kHz. This system is used to characterise the time-dependent, transient magnetic properties of ferrite samples. Results are presented for a commercial NiZn ferrite torus.

Keywords: ferrimagnetic materials, magnetic permeability, magnetic variables measurement, soft magnetic materials, transient magnetic properties, after-effect

## 1 INTRODUCTION

Inductances with NiZn-ferrite cores are commonly used in all sorts of electrical devices for use at frequencies in the MHz range. NiZn-ferrites can avoid eddy current effects due to their high electrical resistivity in the range of $10^5$ Ωm. The preferred shape of the core is usually the ring-core, to realise a closed magnetic circuit, sometimes with a defined small air-gap. If the effective cross-section $A$ of the core is small in comparison to the total magnetic length $l$ of the core, we may additionally assume a homogeneous distribution of flux density $B$ and magnetic field $H$, and consequently a constant permeability $\mu$ of the core. Under these assumptions we can easily calculate *ferrimagnetic material properties* from *electrical AC measurements* of voltage $U$ and current $I$ of a coil with a ferrimagnetic core from Faraday and Ampere laws, with the number of windings $N$

$$U = NA\frac{\partial B}{\partial t},\quad I = H\frac{l}{N} \tag{1}$$

With the total flux $\Phi = A \cdot B$ we define the inductance $L$ of the device as quotient of $\Phi$ and electrical current $I$

$$L = \mu_o \mu_r N^2 \frac{A}{l},\quad \tilde{\mu}_r = \mu_r' - j\mu_r'' \tag{2}$$

The imaginary part of the permeability represents losses.

Ferromagnetic and ferrimagnetic materials, however, are typical examples of non-linear materials, they exhibit saturation and hysteresis. The value of $\mu$ used in the equations above, is not constant, it depends on the course of the hysteresis loop. Ferrite manufacturer's datasheets usually give a value for the initial permeability $\mu_0\mu_i = \mathrm{d}B/\mathrm{d}H$ for vanishing amplitudes of field and flux density (usually for $B < 0.25$ mT), in the origin of the magnetisation loop for $B = 0$ and $H = 0$. Generally, the differential permeability $\mu_0\mu = \mathrm{d}B/\mathrm{d}H$ increases from the value of $\mu_i$ in the origin of the virgin curve until a maximum value around coercivity, and decreases towards 1 for the saturated material. From the engineering point of view, we are interested in the incremental permeability $\mu_0\mu_\Delta = \Delta B/\Delta H$, which is additionally dependent on the respective AC amplitudes $\Delta B$ or $\Delta H$.

If a periodic signal with constant amplitude $\Delta H$ is applied on a ferrimagnetic device, however, several cycles of the signal are needed to establish the closed loop, and the final steady state permeability.

Additionally to the described $B(H)$-hysteresis, which is different for DC conditions and steady-state AC conditions, there is an essential time-dependent effect, a B($t$)-lag, also known as magnetic viscosity or magnetic after-effect. The magnetic after-effect (MAE) [1], [2], [3] describes the delayed change in magnetisation accompanying a sudden change of the magnetic field. This effect can be clearly distinguished from the electromagnetic phenomenon of eddy-currents, and from the irreversible effects of aging or structural change. For AC-magnetisation the after-effect also leads to magnetic losses [4].

In material manufacturer's data-sheets this behaviour is described by a disaccommodation-coefficient $d$ or disaccommodation-factor $DF$ which describe the change of the initial permeability with time, after the material has been carefully demagnetised

$$d = \frac{\mu_{i1} - \mu_i(t)}{\mu_{i1}\log\left(\frac{t}{t_1}\right)},\quad DF = \frac{d}{\mu_{i1}}. \tag{3),(4}$$

* Dept. of Applied Electronic Materials, Inst. of Sensor and Actuator Systems, Vienna University of Technology, Gusshausstr. 27-29, 1040 Wien, Austria.
** Inst. of Electrical Measurement and Measurement Signal Processing, Graz University of Technology, Kopernikusgasse 24/IV, 8010 Graz, Austria.
paul.fulmek@tuwien.ac.at

ISSN 1335-3632 

The disaccommodation-factor *DF* allows to calculate the time dependence of the initial permeability $\mu_i(t)$, if a permeability $\mu_{i1}$ is known at the time $t_1$. There exist many publications dealing with the experimental and analytical investigation of the phenomenology and the physical interpretation of magnetic after-effect (MAE), magnetic viscosity, and sweep-rate dependence. The time-resolution of the well established MAE spectrography (isochronal relaxation curves *vs* temperature, *eg* [5]) is limited to the speed of the used LCR-meters in the range of several measurements per second.

## 2 EXPERIMENTAL SETUP

Our experimental setup determines the magnetic properties of the ring core sample by measuring the signals of current and voltage at the coil, and the respective phase angle of the fundamental harmonic of the signals. Thus the complex impedance of the device can be determined.

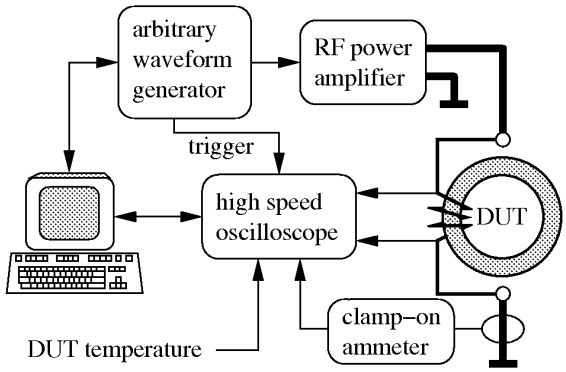


**Fig. 1.** Experimental setup: The generator voltage is applied to the device under test (DUT) by the RF amplifier. A high-speed oscilloscope records the coil voltage, the current, and the temperature of the DUT. The PC controls the system and collects the measured data.

The setup is shown in Fig.1. A programmable arbitrary waveform generator generates the excitation signal and a trigger signal. An RF power amplifier (100 W, 1 GHz bandwidth) feeds the voltage signal to the device under test (DUT). The 4-channel high speed digital storage oscilloscope (DSO, 1 GHz analogue bandwidth) is used to acquire the voltage signal directly at the DUT. The current $I(t)$ is measured by a clamp-on Ampere-meter. Additionally a temperature sensor is mounted on the DUT. The DSO collects the signals from voltage, current, and temperature. The whole system is controlled by a computer. Due to the limited storage capability of the DSO (500 thousand Samples) the measurements are performed in several steps, each acquisition is covering just a fraction of the time of the whole experiment. The trigger-signal of the waveform generator is used to guarantee precise timing for the measurements. Due to different bandwidths and delay times of the components of the setup (cabling, probes, ammeter) the whole system had to be carefully calibrated to guarantee synchronous sampling and reliable, valid timing of the acquired signals. The sampling rate of the DSO is 2.5 GS/s (*ie* 0.4 ns per sample), accordingly the DSO buffer is filled within 200 µs. The buffer data is automatically transferred to the computer, which initiates the next measurement sequence.

A measurement sequence consists of two identical bursts of a 13.5 MHz signal, each burst lasts for 500 ms with a delay of 200 ms between both. The first burst is used to initialise the system; measurements are triggered with reference to the start time of the second burst. This procedure is performed with sequentially shifted trigger times. Figure 2 shows two complete periods of the acquired voltage and current signals.

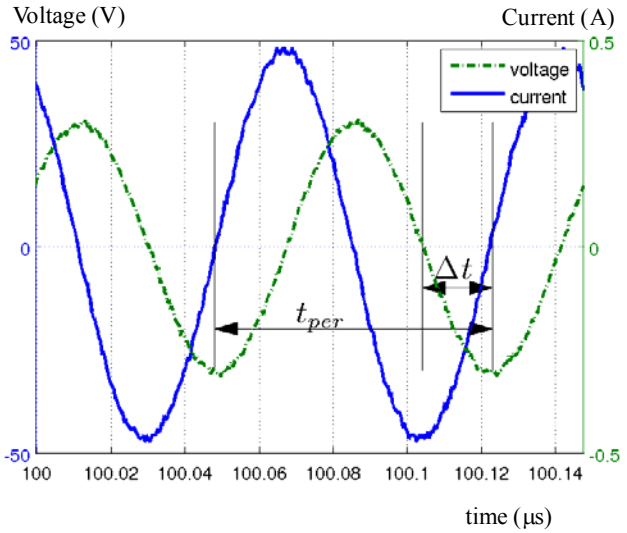


**Fig. 2.** Typical voltage and current signals at a ferrite ring 100 µs after the start of the second burst. The actual signal frequency and the phase shift between voltage and current are determined from $t_{per}$ and $\Delta t$.

After the complete series of experiment is finished, the evaluation of the acquired data is done on the computer. The zero-crossings of the signals are used to determine the approximate period-length and frequency of the signals. The discrete Fourier transform DFT is applied to a sequence of several signal periods and used to find the amplitudes of the spectral components of the signals. From the DFTs of voltage $U(t)$ and current $I(t)$ we determine the complex impedance $\mathcal{Z}$ (absolute value $Z$ and phase angle $\delta$) and the respective components of a series equivalent circuit $\mathcal{Z} = R_L + j\omega L$ for the fundamental harmonic $\omega = 2\pi f$:

$$\begin{aligned} U(t) &= \mathrm{Re}\left\{\mathcal{U}\,\mathrm{e}^{j\omega t}\right\} \\ I(t) &= \mathrm{Re}\left\{\mathcal{I}\,\mathrm{e}^{j(\omega t-\delta)}\right\} \\ \mathcal{Z} &= \frac{U}{I}\mathrm{e}^{j\delta} = R_L + j\omega L \quad . \end{aligned} \tag{5}$$

Figure 3 shows a typical DFT spectrum of an applied voltage signal. After processing the raw measurement signals, the final results for the impedance of the DUT are available with a time resolution of approximately 25 µs. From these results we can extract the complex permeability of the ferrite material sample.

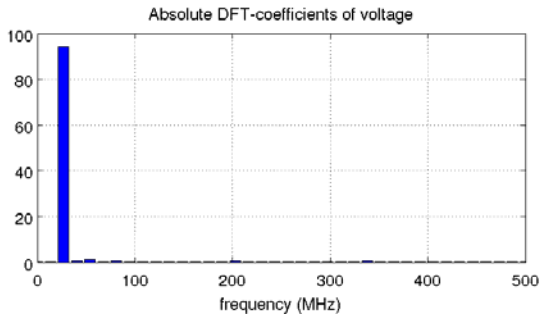


**Fig. 3.** Discrete Fourier Transform of a typical period of the signal. The noise floor level stays below 0.2 % of the fundamental harmonic spectral line.

## 3 EXPERIMENTAL RESULTS

The described measurement setup is used to analyse the behaviour of a toroidal coil with a commercial ferrite core. Such a device is used, *eg*, as antenna transformer for RFID-systems [6], [7]. For every burst of the RF-signal the permeability accommodates to its final value and, consequently, disaccomodates between two bursts. The magnetic properties of the material can be determined almost from the very first beginning of the excitation.

Our sample is a NiZn-ferrite toroid (Ferroxcube 4C65, TN36/23/15) prepared with one set of concentrated copper windings ($N$=3) covering approximately only 10° of the total circumference of the ring. The material properties in Table 1 are taken from the datasheet [8] and [9]. Due to the high specific resistivity no effect of eddy currents should be expected for the used measurement frequency of 13.5 MHz, which is close to a technically important standard RFID frequency (*eg* ISO 15693).

**Table 1.** Ferroxcube 4C65 NiZn ferrite material properties

| | | |
|---|---|---|
| permeability $\mu_i$ | 125 ± 20% | 10 kHz, $B$≤0.25 mT |
| saturation $B_s^*$ | 380 mT | $H_s$ = 3.0 kA/m |
| remanence $B_r$ | 280 mT | |
| coercivity $H_c$ | 280 A/m | |
| loss factor tan$\delta/\mu_i$ | ≤ 130·10$^{-6}$ | 10 MHz, 0.25 mT |
| resistivity $\rho$ | 10$^5$ Ωm | |
| Curie temp. $T_C$ | 350 °C | |

The $A_L$ value in the datasheet almost exactly reflects the result of (2) with the initial permeability $\mu_r = \mu_i$. Accordingly, the expected impedance $j\omega L$ of our sample is about 130 Ω. The number of windings $N$ and the cross-sectional area $A$ of the toroid are exactly determined; the effective magnetic length $l$ has been estimated by FEM simulations and the figures from the data-sheet.

Figure 4 shows the result of the impedance measurements for two different temperatures and levels of the flux-density.

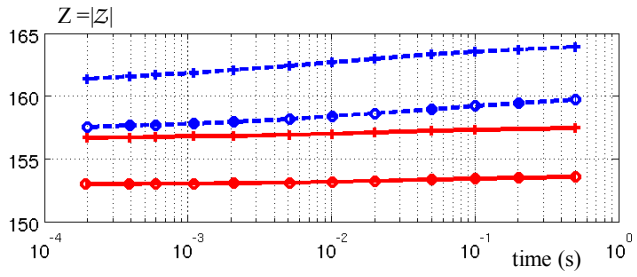


**Fig. 4.** Absolute value $Z$ of impedance *vs* time of the 4C65 ferrite sample. Solid line: $B$ = 1.9 mT, broken line: $B$ = 5.1 mT. Temperature of the core 303 K (+) and 285 K (o).

From several series of measurements we determined the complex permeability from (1), (2), and (5) in dependence of logarithmic time and flux amplitude.

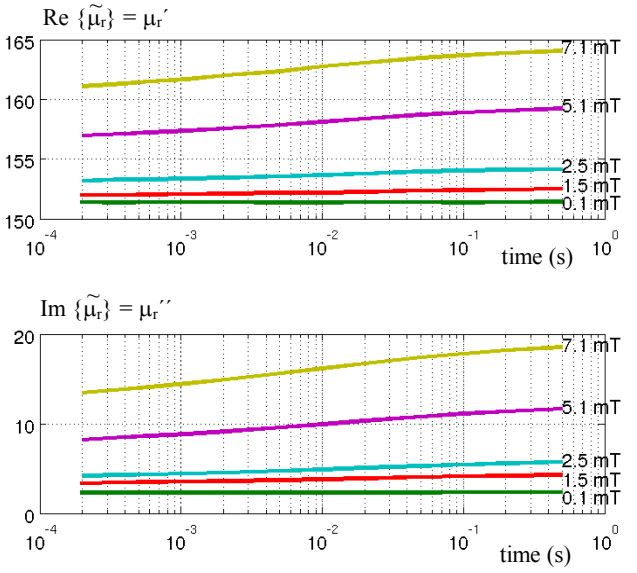


**Fig. 5.** Real and imaginary part of the complex permeability at 302 K, the flux densities range from 0.1 mT (lowest curve) to 7 mT. All measurements show a typical log($t$) characteristic.

Figure 5 shows the complex permeability at a constant temperature of 302 K for different peak levels of the flux density in the range of 0.1-7 mT. During the series of experiments the measured temperature of the core was constant within ± 0.05 °C. A rather linear dependence on logarithmic time can be observed

$$\mu(t) = k \log \frac{t}{t_0} + \mu(t_0) \qquad (6)$$

The factor of proportionality $k$ compares to the expression for the initial permeability $\mu_{i1} \cdot d$ as given in (3), and

shows dependence on the temperature and on the peak value of the flux-density.

From these results we have determined the coefficients of the log($t$) characteristic, the time constant $t_0 = 1$ s has been chosen. Fig.6 shows the dependence of the coefficients in (6) from peak flux density and temperature. The factor $k$ appears to depend linearly on $B$, whereas the coefficient $\mu(t_0)$ depends on the squared induction:

$$k = f\left(B,T\right), \quad \mu(t_0) = f\left(B^2,T\right) \tag{7}$$

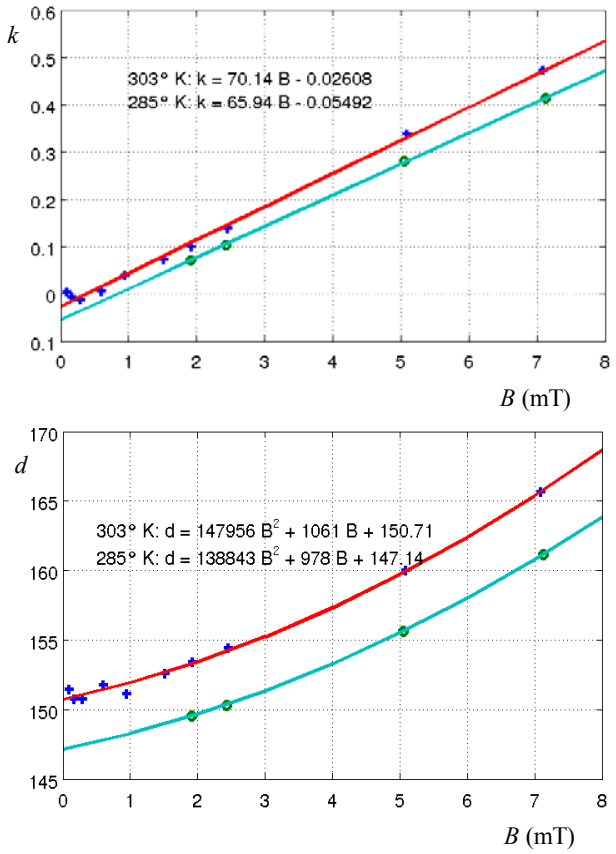


**Fig. 6.** Coefficients $k$ (top) and $d$=$\mu(t_0)$ (bottom) of the equation $|\mu| = k \log(t/t_0) + |\mu(t_0)|$ in dependence of peak induction $\hat{B}$ for temperatures of 285 K (o) and 303 K (+). Additionally the linear and quadratic fit-functions are displayed for both temperatures.

## 4 CONCLUSION AND OUTLOOK

We have presented a measurement system to determine the change of magnetic properties with time in the range of µs, and experimental results for the magnetic accommodation effects of a NiZn-ferrite ring coil. During a repeatedly applied sequence of 13.5 MHz bursts the complex impedance of the coil is sampled by a high-speed measurement system. The behaviour can be described by the typical log($t$)-dependence of the complex permeability, with coefficients varying with temperature and the applied flux density. Up to a peak flux density of 5 mT no considerable temperature variation occurred during the measurement series, the temperature could be held constant.

To reliably define a reasonable quantitative functional dependence of the magnetic accommodation on induction and temperature [10] more experimental results at different temperatures are necessary. Besides, the MAE phenomena need to be clearly distinguished from the pseudo-time-dependence of the evolution of minor loops towards closed minor loops (*eg* Rayleigh loops), which happens at DC, as well. The measurement of the DC magnetisation, the DC operating point in the $B(H)$-loop will be required, additionally.

**Acknowledgement**

The authors gratefully announce the financial support of the Austrian Science Fund (FWF) under the reference number L356-N14.

## REFERENCES

[1] PREISACH, F.: Über die magnetische Nachwirkung, Z. Physik **94** (1935), 277–302

[2] NÉEL, L.: Théory du traînage magnétique des substances massives dans le domaine de Rayleigh, J. Phys. Rad. **11** No. 2 (1950), 49

[3] NÉEL, L.: Le traînage magnétique, J. Phys. Rad. **12** (1951), 339–351

[4] CHIKAZUMI, S.: *Physics of Magnetism*, John Wiley & Sons, Inc., New York – London – Sidney (1964)

[5] FRANCISCO, C. – INIGUEZ, J. I. – MUNOZ, J. M. – AYLA, J.: Automatic disaccommodation measuring system, IEEE Trans. Magn. **23** No. 2 (1987), 1866–18689

[6] FULMEK, P. – HAUSER, H. – STEINER, G: - HAUMER, P.: Magnetic modelling of continuously variable transformers, Physica B **372** (2006), 124–127

[7] STEINER, G. – ZANGL, H. – FULMEK, P. – BRASSEUR, G.: A tuning transformer for the automatic adjustment of resonant loop antennas in RFID systems, *International Conference on Industrial Technology ICIT04* (2004)

[8] Ferroxcube – A Yageo Company: Datasheet – 4C65 Material Specification (Sept. 2008)

[9] Philips Components: Product Specification – Ferrite Ring Cores – TN36/23/15 (Nov. 1997)

[10] DELLA TORRE, E. – BENNET, L. H.: Temperature variation of magnetic aftereffect, IEEE Trans. Magn. **37** No. 3 (2001), 1118–1122

Received 30 September 2010